



## UHI Research Database pdf download summary

### Parallelisable non-invasive biomass, fitness and growth measurement of macroalgae and other protists with nephelometry

Calmes, Benoît; Strittmatter, Martina; Jacquemin, Bertrand; Perrineau, Marie-mathilde; Rousseau, Céline; Badis, Yacine; Cock, J. Mark; Destombe, Christophe; Valero, Myriam; Gachon, Claire M.m.

*Published in:*  
Algal Research

*Publication date:*  
2020

*The re-use license for this item is:*  
CC BY-NC-ND

*The Document Version you have downloaded here is:*  
Peer reviewed version

*The final published version is available direct from the publisher website at:*  
[10.1016/j.algal.2019.101762](https://doi.org/10.1016/j.algal.2019.101762)

### [Link to author version on UHI Research Database](#)

*Citation for published version (APA):*

Calmes, B., Strittmatter, M., Jacquemin, B., Perrineau, M., Rousseau, C., Badis, Y., Cock, J. M., Destombe, C., Valero, M., & Gachon, C. M. M. (2020). Parallelisable non-invasive biomass, fitness and growth measurement of macroalgae and other protists with nephelometry. *Algal Research*, 46, Article 101762. Advance online publication. <https://doi.org/10.1016/j.algal.2019.101762>

#### General rights

Copyright and moral rights for the publications made accessible in the UHI Research Database are retained by the authors and/or other copyright owners and it is a condition of accessing publications that users recognise and abide by the legal requirements associated with these rights:

- 1) Users may download and print one copy of any publication from the UHI Research Database for the purpose of private study or research.
- 2) You may not further distribute the material or use it for any profit-making activity or commercial gain
- 3) You may freely distribute the URL identifying the publication in the UHI Research Database

#### Take down policy

If you believe that this document breaches copyright please contact us at [RO@uhi.ac.uk](mailto:RO@uhi.ac.uk) providing details; we will remove access to the work immediately and investigate your claim.

**Short title: Nephelometry for algal and protistan phenomics**

**Corresponding author details:** Claire M.M. Gachon

Scottish Association for Marine Science, Scottish Marine Institute, PA37 1QA Oban, United Kingdom

Tel: 0044 16 31 559 318.

**Title:** Parallelisable non-invasive biomass, fitness and growth measurement of macroalgae and other protists with nephelometry

**Author names and affiliations**

Benoît Calmes<sup>1,2</sup>, Martina Strittmatter<sup>1,3</sup>, Bertrand Jacquemin<sup>2,4</sup>, Marie-Mathilde Perrineau<sup>1</sup>, Céline Rousseau<sup>5</sup>, Yacine Badis<sup>1,6</sup>, J. Mark Cock<sup>6</sup>, Christophe Destombe<sup>2</sup>, Myriam Valero<sup>2</sup>, Claire M.M. Gachon<sup>1,7</sup>

Declarations of interest: none

**Present addresses:**

<sup>1</sup>: Scottish Association for Marine Science, Scottish Marine Institute, PA37 1QA Oban, United Kingdom

<sup>2</sup>: CNRS, UMI 3614, Sorbonne Université, Pontifica Universidad Catolica de Chile, Universidad Austral de Chile, Place Georges Teissier, CS90074, 29688 Roscoff, France

<sup>3</sup>: Sorbonne Université, CNRS, ECOMAP team, UMR 7144, Adaptation and Diversity in the Marine Environment, Station Biologique de Roscoff, CS 90074, F-29688, Roscoff, France

<sup>4</sup>: Centre d'Etude et de Valorisation des Algues, Presqu'île de Pen Lan, 22610 Pleubian, France

<sup>5</sup>: PHENOTIC, SFR 4207 QUASAV, Angers, France

<sup>6</sup>: Sorbonne Université, CNRS, Algal Genetics Group, UMR 8227, Laboratory of Integrative Biology of Marine Models, Station Biologique de Roscoff, CS 90074, F-29688, Roscoff, France

<sup>7</sup>: Muséum National d'Histoire Naturelle, CNRS, UMR 7245 - Molécules de Communication et Adaptation des Micro-organismes , CP 54, 57 rue Cuvier, 75005 Paris, France

**Corresponding author e-mail:** [claire.gachon@sams.ac.uk](mailto:claire.gachon@sams.ac.uk)

## **Abstract**

With the exponential development of algal aquaculture and blue biotechnology, there is a strong demand for simple, inexpensive, high-throughput, quantitative phenotyping assays to measure the biomass, growth and fertility of algae and other marine protists. Here, we validate nephelometry, a method that relies on measuring the scattering of light by particles in suspension, as a non-invasive tool to measure in real-time the biomass of aquatic micro-organisms, such as microalgae, filamentous algae, as well as non-photosynthetic protists. Nephelometry is equally applicable to optic density and chlorophyll fluorescence measurements for the quantification of some microalgae, but outperforms other spectroscopy methods to quantify the biomass of biofilm-forming and filamentous algae, highly pigmented species and non-photosynthetic eukaryotes. Thanks to its insensitivity to the sample's pigmentation, nephelometry is also the method of choice when chlorophyll content varies between samples or time points, for example due to abiotic stress or pathogen infection. As examples, we illustrate how nephelometry can be combined with fluorometry or image analysis to monitor the quantity and time-course of spore release in fertile kelps or the progression of symptoms in diseased algal cultures.

## **Keywords**

algal cultivation; nephelometry; biomass; phenotyping; biotechnology

## 1. Introduction

Underpinned by strong economic and political drivers such as food safety, blue biotechnology and transition to a low carbon economy, macroalgal cultivation is the fastest growing of all aquaculture sectors worldwide, with a sustained exponential growth attaining almost 10% in value annually. Beyond their traditional use as sea vegetables, macroalgae are increasingly used as animal feed and for hydrocolloids, biofuels, bioplastics and pharmaceuticals [1, 2]. Over the last few years, genomic resources for marine macroalgae have been established, especially for the filamentous brown alga *Ectocarpus siliculosus* [3], the carrageenophyte *Chondrus crispus* [4] and more recently, the kelp *Saccharina japonica* [5]. First initiated in China in the 1950s, industrial macroalgal breeding led to the development of kelp cultivars with increased yield and iodine content ([6] and references included). Over the last decades, seaweed aquaculture has rapidly spread to most continents, leading to the ongoing rapid domestication of several dozen species [7]. Cultivar development however remains largely empirical [8]. For the vast majority of species, wild genetic resources are at best poorly characterised, and their exploitation is therefore very limited [9]. Thanks to second generation sequencing technologies, characterising this diversity is now technically within reach and accordingly, demand for marker-assisted breeding tools is booming [e.g. 10]. However, the implementation of quantitative trait loci (QTL) or genome-wide association studies (GWAS) is slowed down by the limited availability of effective high throughput, quantitative phenotyping methods for traits of interest.

In land agriculture, phenomics is now a well-established field that underpins selection and breeding; high throughput phenotyping facilities have become mainstream and typically combine, parallelise and automate various hyperspectral or temporally-resolved imaging techniques. In aquatic sciences, lab-based high-throughput quantitative phenotyping is to some extent available thanks to sizing and sorting technologies such as Coulter counters and flow cytometers [11], coupled to image analysis (e.g. FlowCam). Thus far, unicellular microalgae have typically been models of choice whenever large-scale phenotyping efforts are required, such as for conducting genetic screens [e.g. 12]. In sharp contrast, high-throughput phenotyping tools for multicellular aquatic organisms, including

macroalgae, are very much lagging behind, including in the submillimetric to centrimetric size range. In particular, due to the highly hygroscopic nature of macroalgal cell walls, there is no simple way to accurately measure the fresh weight, let alone to follow the growth of seaweed non-invasively. As a result, total chlorophyll fluorescence (or parameters such as  $F_0$ , the minimal chlorophyll fluorescence under non-actinic light) and spectrophotometry are often used as proxies for measuring the biomass of algae (Fig. 1A-B). However, fluorescence measurements are inherently sensitive to variations in chlorophyll content linked to environmental factors such as stress, nutrient supply or light conditions, i.e. the very variables that are typically most relevant to breeders and ecologists alike. Spectrophotometry is equally unsatisfactory for measuring thick, opaque samples such as seaweed tissue and is sensitive to the sample pigmentation, a limitation particularly relevant when biomass measurements are needed in the context of disease monitoring.

In flow cytometers, the measurement of the light scattered by particles in suspension is widely used to assess the size and biomass of live cells [e.g. 13], yet such measurements can only be conducted on single cells with a maximum diameter of ca. 30  $\mu\text{m}$ . Nephelometers (Fig. 1C) also rely on the measurement of scattered light and are commonly used in aquatic ecology to measure water turbidity (i.e. combined plankton and sediment content). In chemistry, another application is to follow in real time the solubilisation of fine particles or analyse ligand-binding responses, for example in immunoassays. More anecdotally, the radiation properties of microalgae have been explored with nephelometry, within the context of optimising photobioreactor design [14]. Recently, we demonstrated the applicability of nephelometry to monitor the growth of filamentous phytopathogenic fungi such as *Botrytis*, *Aspergillus* and *Alternaria* [15-17]. The potential of this technique for quantifying algal biomass was already recognised over forty years ago [18]. However, the instruments available at that time only allowed to measurement of one sample at a time and with a fairly low sensitivity, hence the technique was never widely adopted. Nowadays, significant design improvements have increased the sensitivity of nephelometers and reduced the variability of measurements and the availability of microplate readers allows for the necessary the automation and

replication required for medium- to high-throughput analyses. Here, we assessed the applicability of using a microplate-format nephelometer to monitor in real time and non-invasively the biomass of algae and other aquatic protists.

## 2. Materials & Methods

### 2.1. Strains and cultivation media

Clonal partheno-sporophytes of the fully sequenced, male *Ectocarpus siliculosus* strain CCAP 1310/4, clonal female gametophytes of the *Macrocystis pyrifera* strain CCAP 1323/1 and the obligate biotrophic oomycete *Anisolpidium ectocarpii* strain CCAP 4001/1 were maintained as previously described at 15°C, under a 12:12 light:dark photoperiod and low white light intensity of 2  $\mu\text{mol photons m}^{-2} \text{s}^{-1}$  [19, 20]. These low light conditions are optimised to facilitate the maintenance of the pathogen. Whereas healthy *E. siliculosus* and *M. pyrifera* both grow at such low light levels, their development is much faster under an irradiance of 20  $\mu\text{mol m}^{-2} \text{s}^{-1}$ . Cultures were transferred into fresh half-strength Provasoli enriched seawater medium every 3 weeks and monitored on a weekly basis by microscopy. Whenever homogeneity of the biological material was paramount (e.g. for serial dilutions), the algal filaments (*E. siliculosus*, *M. pyrifera*) were finely disrupted with a sterile Potter tissue grinder, and allowed to regenerate for 2-3 weeks before being measured.

The microalgae *Haematococcus pluvialis*, *Micromonas* sp. (RCC3510), *Emiliania huxleyi* (RCC3553), *Phaeocystis* sp., *Alexandrium minutum* (RCC1490), *Guinardia flaccida* (RCC3088) were kindly gifted by the Roscoff Culture Collection. The axenic *Paraphysoderma sedebokerense* strain PS1 was sub-cultured every 3-4 weeks to fresh liquid chytrid growth medium as detailed in Strittmatter *et al.* [21]. A mono-eukaryotic chytrid strain of *Zygorhizidium effluens* isolated during a bloom of its freshwater diatom host, *Asterionella formosa*, was grown in diatom medium, at 20°C under a 12h photoperiod and irradiance of 60  $\mu\text{mol m}^{-2} \text{s}^{-1}$  [22]. A suspension of chytrid zoospores was obtained by filtration of an infected culture on a 10  $\mu\text{m}$  pore size nylon membrane. The calibration curves obtained by serial dilution in fresh or seawater, as appropriate (biological replicate, n=3).

Two *Saccharina latissima* unfertile sporophytes (named A and B) were sampled in the port of Roscoff (France) and 28x14cm pieces of the blades were cultivated under controlled conditions (8:16 light:dark photoperiod; flowing filtered seawater at 13°C) until the appearance of fertile sori occurred. To trigger spores release, two fragments (0.5x3cm) of sorus were cut with a scalpel from each of the two sporophytes and allowed to air-dry for 8 hours in the dark at 13°C. The fragments were then carefully bent and disposed vertically against the inner side of individual wells in a 24-well plate, outside the central area measured by the nephelometer and submerged in 2 mL of filtered and sterilised seawater (inset on Fig. 8D).

## 2.2. Nephelometric measurements and data analysis

Sterile 96 UV-star, 48 and 24 cell culture Greiner microplates were filled with 300 µL, 1 mL and 2 mL samples, respectively. Nephelometric measurements were recorded with a NEPHELOstar Omega (BMG Labtech, Offenburg) reader equipped with a 635 nm laser. Each well was measured for 0.1 s with a laser beam focus of 2.5 mm and 80% laser intensity.

Filaments and clumps of *E. siliculosus*, *M. pyrifera*, *H. pluvialis*, *P. sedebokerense*, *P. littoralis* data were measured using a well-scan protocol and a 5x5 pixel grid covering 5 mm in diameter (48-well microplates) or a 7x7 pixel grid covering 10 mm diameter (24-well microplates). Spores of *S. latissima* and other microalgae were measured using an endpoint protocol. The time-course of *S. latissima* spore release was recorded using a time-course of endpoint (plate mode) protocol, during which the 24-well plates were subjected to shaking at 175 rpm for 5 min every 10 min.

To check for the possible presence and subsequently control for any artefact caused by a meniscus in the nephelometric well scans, the data analysis was conducted on the average measurement recorded in a centred disc of 3.5 mm diameter using the corresponding function in the Mars software (BMG Labtech, Offenburg). CSV files were exported and further processed in Microsoft Excel and R [\[23\]](#). Regression curves were compared using the ANCOVA test implemented in Graphpad Prism 7. At all times, the background signal was measured in duplicate using appropriate mock samples, and the



corresponding mean values were subtracted from all measurements. For time courses, an initial relative nephelometric unit (RNU) value was calculated as the mean of the initial three measurements and then subtracted from each curve value as described by Joubert *et al.* [15].

### **2.3. Spectrophotometry and Fluorometry**

For comparative purposes, absorbance and fluorescence data were recorded on the samples used in nephelometry using a SPECTROstar Omega (BMG Labtech, Offenburg). The recording wavelength (450 nm or rarely, 250 nm) was selected to give the most sensitive measurements, depending on the species used. Chlorophyll fluorescence was recorded using a 12 nm band pass excitation filter, centred on 485 nm, and a 50 nm band pass emission filter, centred on 655 nm. Unless specified otherwise, all experiments were performed on at least three (and up to six) biological replicates, each composed of 3 technical replicates.

### **2.4. Dry weight measurements**

A serial dilution of *E. siliculosus* tufts (three technical replicates per concentration) was analysed using nephelometry, spectrophotometry and fluorometry before dry weight was determined. Due to the small amounts of biomass used, the *E. siliculosus* fragments contained in the three technical replicates were pooled, oven-dried overnight and then weighed three times with a precision scale (Sartorius, Secura 225D-1S, d=0.00001g).

### **2.5. Image analysis**

The reproductive effort of kelp sporophytes was evaluated as a function of the percent blade area occupied by sori (De Wreede & Klinger, 1988). The blade fragments were photographed; the fertile area (slightly swollen dark spots) showed the highest contrast with the vegetative part of the thallus in the red frame of the RGB image, which was thus used for analysis. The red frame was segmented as described in Rousseau *et al.* [24]: briefly, the distribution of pixel intensity was plotted for a

manually-identified unfertile area, in order to determine the signal intensity threshold under which the red channel intensity could be assigned to a sorus; we determined that setting the threshold to the maximum red channel intensity of the lower 2<sup>nd</sup> percentile of vegetative pixels gave best results. All images were then processed and split using this threshold, with all pixels automatically split between the dark (fertile) and bright (vegetative) areas.

## **2.6. Microscopy**

Algal material was observed directly in the multiwell plates with an AxioObserver (Zeiss) microscope, using differential interference contrast and phase contrast. For epifluorescence, culture aliquots were mounted on microscope slides. Photographs were taken using an AxioCam HRc (Zeiss) and processed with Axiovision software (Zeiss, version 4.7 or 4.8).

## **3. Results**

### **3.1. Comparison of fluorometry, spectrophotometry and nephelometry for non-invasive quantification of algal and non-photosynthetic eukaryote biomass.**

The performance of nephelometry, fluorometry and optical density to measure the biomass of micro- and macroalgae and non-photosynthetic eukaryotes was benchmarked against dry weight measurement. The excitation (12 nm band pass, centred on 485 nm) and emission (50 nm band pass, centred on 655 nm) wavelengths of the fluorimeter were chosen to capture a proxy of the total chlorophyll content.

A sample of *E. siliculosus* filaments was measured ten times with each of the three methods in order to assess the reproducibility of measurements. The standard deviation was around 5% for the fluorimeter and nephelometer but as high as 22% with spectrophotometry, despite the fact that the recorded wavelength (440 nm) had been chosen to maximise the signal/noise ratio. Therefore, optical

density (OD) appears less adapted to estimate algal biomass, at least on filamentous algae such as *E. siliculosus* (Fig. S1).

Using a serial dilution of *E. siliculosus* filaments, we then measured the degree of agreement between dry weight, nephelometry, fluorometry and spectrophotometry measurements. As expected, dry weight measurements were highly correlated to the dilution factor applied ( $r^2 = 0.9786$ , Fig. 2A) and the slope of the linear regression curve had a negligible variation compared to the expected one (1.0%). However, some variability was apparent for the lowest biomass containing samples. Additionally, the length and destructiveness of the dry weight protocol make it unsuitable for phenomic applications. As judged from the linearity ( $r^2 = 0.9933$  and  $0.9817$ , respectively) and slope deviation (2.8% and 1.0%, respectively), nephelometry and spectrophotometry performed best amongst the three light-based methods tested (Fig. 2B). Fluorometry measurements betrayed a lower sensitivity for low quantities of biological material, and thus showed some deviation from linearity ( $r^2 = 0.9711$ ) and proportionality (5.5%, Fig. 2C).

To test the generality of the above findings, the linearity of the nephelometric, fluorometric and spectrophotometric readings was further tested on different algal and protistan species, encompassing a broad range of morphologies, mobile or biofilm-forming properties and pigment content. For each species, calibration curves were built as described in Fig. 2 and the  $r^2$  of the resulting linear fit was plotted (Fig. 3). With  $r^2$  values equaling at least 0.97, all three methods yielded satisfactory standard curves for a variety of microalgae (*Micromonas* sp., *Emiliana huxleyi*, *Haematococcus pluvialis*, *Alexandrium minutum* and *Guinardia flaccida*). However, the calibration curve obtained with spectrophotometry was poor for highly pigmented (*Macrocystis pyrifera*,  $r^2=0.739$ ) and biofilm-forming (*Phaeocystis* sp.,  $r^2=0.927$ ) biological material; for these two species, fluorometry also gave slightly lower  $r^2$  values compared to nephelometry (0.929 vs. 0.989 for *M. pyrifera* and 0.900 vs. 0.981 for *Phaeocystis* sp. respectively). Predictably, fluorometry was inadequate to measure the biomass of non-chlorophyllous species ( $r^2 = 0.026$  and  $0.076$  for *Paraphysoderma sedebokerense* and *Zygorhizidium effluens*, respectively). In comparison, OD measurements led to a

much better  $r^2$  of 0.943 for *P. sedebokerense*, yet the spectrophotometer struggled to pick up a meaningful signal with low concentrations the *Z. effluens* spore suspensions, resulting in a poor  $r^2$  of 0.386. For both chytrid species, the best calibration curves were obtained with nephelometry, as shown by  $r^2$  values of 0.974 (*P. sedebokerense*) and 0.963 (*Z. effluens*).

### 3.2. Non-invasive monitoring of algal growth

The growth of *E. siliculosus* filaments was followed in 48-well plates over 13 days (Fig. 4). As expected from Fig. 2, all three techniques gave measurements roughly consistent with each other, and spectrophotometry measurements were noisier. Note also that the initial fluorometric measurement was below the value of a blank sample (i.e. below the detection threshold of the machine), whereas the last time point was saturated. This illustrates how the narrower dynamic range of this technique hampers long-term monitoring of a culture, a limitation that was not encountered when nephelometry or spectrophotometry were used. Additionally, we evaluated how the three techniques discriminated between mild growth variations during hyposaline stress, while also testing the impact of physiologically-significant variations in chlorophyll content by exposing cultures to increased light levels ( $20 \mu\text{mol m}^{-2} \text{s}^{-1}$  vs.  $2 \mu\text{mol m}^{-2} \text{s}^{-1}$  in the control; Fig. 5). At five days, nephelometry and spectrophotometry detected a significant increase in biomass in response to increased illumination compared to the standard illumination regime, with fold increases of 1.3 and 1.6. However, a strikingly different pattern was observed with fluorometry: between the first and second day of the time course, the total fluorescence soared from below 1kRFU to 32 kRFU. Daily observation of the microplates by the experimenters ruled out the possibility that such a sudden overnight increase corresponded to a commensurate biomass increase, and was therefore attributed mainly the induction of chlorophyll synthesis due to photoacclimation [see [25](#), [26](#)]. Subsequently, the fluorescence readings remained at least one order of magnitude higher in the  $20 \mu\text{mol.m}^{-2}.\text{s}^{-1}$  condition compared to the low light control until the end of the experiment (Fig. 5B). For example, we recorded 1.8kRFU for the control and 47kRFU under increased light at 5 days, suggesting far higher fold changes than those recorded by

nephelometry and OD. Therefore, we conclude that the meaningful biomass changes detected with spectrophotometry and nephelometry were entirely obscured in fluorometry by the co-occurring photoacclimation. Taking into account the general agreement between nephelometry and spectrophotometry data, the complete insensitivity of nephelometry to pigmentation (see next section) and the noisiness of OD measurements (Fig. S1), we conclude that nephelometry is the most accurate technique to follow non-invasively *E. siliculosus* growth over time, across different culture conditions. Similarly, nephelometry proved useful to follow the growth of several macro and microalgae species as well as the non-photosynthetic *P. sedebokerense*, over time periods ranging from 3 days to 2 weeks (not shown).

### **3.3. Diagnosis and monitoring of the progression of symptoms in diseased algal cultures.**

As light scattering by particles is insensitive to pigmentation, we reasoned that nephelometry should be blind to the accumulation of dead algal cells in diseased cultures. To confirm this hypothesis, calibration curves were obtained with *E. siliculosus* filaments before and after being killed, with 1% sodium hypochlorite (i.e. a five-fold dilution of a commercial 5% bleach solution, Fig. 6). The nephelometric standard curve for the dead biomass remained indistinguishable from the one obtained before treatment ( $p=0.62$ ), despite the complete loss cell content of the algal filaments (Fig. 6D-E); the fluorescence of bleach-treated biomass flat-lined across the whole concentration range tested. With spectrophotometry, the slope of the calibration curve for the bleached samples was roughly halved compared to the live control, illustrating again that OD measurements co-vary with both sample biomass and pigmentation.

We exploited the insensitivity of nephelometry to the physiological status of the algae to monitor symptom progression in algal cultures infected by pathogens. As an example, Fig. 7A-C shows the evolution of the nephelometry, fluorometry and spectrophotometry values recorded for gametophytes of the Pacific kelp *M. pyrifera* inoculated with the intracellular oomycete pathogen *Anisolpidium ectocarpii* CCAP 4001/1 [[see details in 20](#)]. Microscopic observation of symptoms

revealed that most algal filaments were dead within three days of inoculation, which was visibly accompanied by loss of chlorophyll fluorescence in infected and dead cells (Fig. 7D-E). Macroscopically, the infected algae exhibited a depigmentation similar to the one observed with sodium hypochlorite. The arrest of algal growth in infected cultures was detected in the nephelometric measurements over the time course, whereas the uninfected control grew steadily up until the end of the experiment (Fig. 7A). In contrast, total chlorophyll fluorescence values went down in the infected samples after two days (Fig. 7B). Consistent with our earlier observations, OD measurements were noisy and difficult to interpret, because the conjugated effects of depigmentation and growth arrest could not be disentangled (Fig. 7C). Therefore, and provided all other factors likely to affect intracellular chlorophyll content are controlled for (e.g. light regime), normalising chlorophyll fluorescence over nephelometric measurements would be a cost-effective and non-invasive way to monitor disease progress in defined algal pathosystems, thus providing a high-throughput alternative to scoring symptoms with microscopy.

#### **3.4. Quantification of macroalgal fertility**

The life cycle of kelps alternates a diploid macroscopic sporophyte with haploid dioecious gametophytes. The sporophytes produce meiospores in one specialised part of the blade called the sorus. After release, the spores differentiate in either male or female gametophytes, by which fertilization give a new sporophyte. One main challenge in the study of the fertility for the diploid phase, is the estimation of the total area occupied by the sori and the average number of spores to be produced and released. To demonstrate the feasibility of fertility measurements, we evaluated the number of spores released by kelp sporophytes through the combined measurement of their fertile area with image analysis, and of the spore release by unit of surface and time, using nephelometry. Firstly, fertile sporophytes of *Saccharina latissima* were photographed in rudimentary lighting conditions, close to those that might be encountered in the field (Fig. 8A). The sori have a darker pigmentation than the vegetative parts of the thallus, allowing for a threshold to be set in order to

distinguish between fertile and vegetative tissue. The picture shown in Fig. 8A was thus segmented to determine the percentage of pixels corresponding to the totality of the sporulation area (Fig. 8B); in this particular example the sorus covered 45.36% of the photographed area. Visual inspection showed that the proportion of pixels misclassified as a result of the shadows projected on the uneven surface of the kelp was negligible. Therefore, image analysis could easily be automated to measure the fertile areas of kelps, both in the laboratory and in the field.

Secondly, spores were collected from fragments of *S. latissima* sori incubated overnight in the dark at 200 rpm in sterile seawater. The spore suspension was calibrated with a Malassez cell, serially diluted in triplicates, and measured by nephelometry and spectrophotometry (Fig. 8C). A linear relationship between the number of *S. latissima* spores and the nephelometric units ( $r^2= 0.997$ ) was found for concentrations ranging from  $10^4$  to  $10^6$  spores  $\text{mL}^{-1}$ . Finally, spore release was monitored in real-time using nephelometry (Fig. 8D). Fertile areas were cut with a scalpel (0.5x3cm) in duplicates, from two individuals named A and B. At the end of the 150 min measurement period, we determined that, on average, the sori of individuals A and B released  $9.76 \cdot 10^5$  and  $5.13 \cdot 10^5$  spores  $\text{cm}^{-2}$ , respectively.

#### **4. Discussion**

Here, we piloted nephelometry as a precise, non-invasive method to carry out biomass and growth measurements with algae and other aquatic eukaryotes. In all experiments, nephelometry always performed at least equally well and often outperformed spectrophotometry and/or fluorometry, in terms of reproducibility, response linearity, sensitivity, and dynamic range. Among the three non-invasive light-based methods tested, nephelometry and spectrophotometry came closest to destructive, end-point dry weight measurements in terms of accuracy. Our results are consistent with the findings of Chioccioli *et al.* [27], who found that spectrophotometry was less reliable and noisier than light scattering measurement in a flow cytometry assay designed to measure microalgal biomass; note however that our approach is considerably simpler than that of Chioccioli *et al.* [27]. For non-invasive monitoring of microalgae and non-photosynthetic protists alike, nephelometry offers a fast

and sensitive alternative to painstaking cell counts [e.g. 28] or flow cytometry, at a fraction of the cost. In addition, the possibility to use 6-well microplates makes the technique applicable to aquatic macroorganisms up to a centrimetric size, the growth of which could thus far not easily be monitored. Using a treatment with sodium hypochlorite, we experimentally confirmed that nephelometry measurements are insensitive to sample discolouration. Therefore, we conclude that nephelometry delivers true, rapid, inexpensive and non-invasive measurements of total biomass, irrespective of the organism's pigmentation or physiological status. Note however that a potential drawback of the apparatus blindness to pigmentation is that measurements are sensitive to the presence of unwanted particles, such as contaminating microorganisms, any precipitate or sediment. Whereas the technique is suitable to monitor pure laboratory cultures, caution with data interpretation should be applied when working with species mixes or environmental samples.

Nephelometry therefore offers an attractive alternative to the widely-used assays that rely on OD, total chlorophyll or  $F_0$  measurements as a proxy for biomass [e.g. 29]. As shown here, physiologically-relevant variations in chlorophyll content, such as photoacclimation or pathogen-induced cell death, may result in fluorescence readings not being strictly proportional to biomass, in addition to being sensitive to cell aggregation [30]. Whereas fluorometry appears adequate to compare biomass variations on the short term, or to compare differences between dilutions of a single sample, our data beg into question the validity of using  $F_0$  or chlorophyll fluorescence to follow biomass variations over several days.

The microplate format of the Nephelostar reader allows easy combination with other plate readers (e.g. fluorometer), to relate sample biomass to physiological parameters (e.g. total chlorophyll fluorescence). Combined with fluorescence (total chlorophyll, or any other parameter measurable with pulse amplitude modulated fluorometry), nephelometry is therefore the method of choice to quantitatively assess the effects of abiotic stress (e.g. light regime, temperature, nutrient limitation, exposure to a pollutant) or biotic stress on micro- and macroalgae. Additionally, the microplate format also allows for the parallelisation and automation required for phenomics experiments. This opens



the perspective of developing fast, medium-throughput, quantitative assays to support the development of QTL and genome wide association studies on models such as *Ectocarpus* [31], and breeding initiatives on commercially important species such as kelps [10, 32]. The statistical power of QTL or GWAS studies increase with the experimenter's ability to simultaneously analyse multiple traits of interest [e.g. 33]. For example, disease monitoring in *E. siliculosus* or other filamentous brown algae currently relies on time-consuming microscopy, which requires highly trained staff, or end-point measurement of relative pathogen and algal abundance with real-time PCR [19]. We are currently piloting disease monitoring assays, that combine nephelometric measurements with pathogen detection using cell-wall stains like Calcofluor white [for the detection of chytrids or of some oomycetes, 20, 34] or specific, fluorescently-labelled lectins [for some oomycetes, 35]. In parallel, chlorophyll fluorescence and quantum yield may be monitored for the simultaneous, real-time measurements of growth, pathogen prevalence, and algal disease tolerance, respectively.

As different type of possible application, we show that combining image analysis with nephelometry provides a rapid and simple estimation of the reproductive effort of kelp sporophytes, with minimal damage to the plants. Evaluating of the fitness in kelps species is a main challenge because fitness is related to the growth and the fertility of both the sporophytes and gametophytes. While morphological traits are easily measured on macroscopic sporophytes, our growth data *E. siliculosus* open interesting perspectives to monitor the growth of gametophytes and young sporophytes. Second, our real-time quantification of spore release shows that nephelometry is applicable to characterize the reproductive traits of propagules (i.e. spores or gametes), release, opening the prospect of exploring both sporogenesis and gametogenesis. Although we did not explore this feature here, the time-course of propagule release could easily be monitored, for example depending on environmental factors.

This new approach would have immediate applications for crop improvement, or could be also used to address outstanding questions in evolutionary genetics: for example, seaweeds are characterized by a unique variability of life cycles, ranging from diploid through haploid-diploid to haploid life cycles

[36, 37]. Despite considerable theoretical work, there is still no unequivocal explanation for the existence and stability of such a large diversity of life history traits [38]. To address this question, reliable estimates of individual fitness in the field and/or in the lab are required [39]. Such experiments can now be planned to compare the fitness of the haploid and diploid life stages using nephelometry. In the long term, the versatility and potential applications of microplate-format nephelometers for macroalgal and protistan biomass monitoring is probably best illustrated by the current diversity of flow cytometry assays that rely on light-scattering measurements [e.g. 40]. Novel specific applications of nephelometry might encompass the investigation of phototrophic biofilms, which are typically made of heterogeneous mix of bacteria and microalgae. Also, combining fluorometry and nephelometry might enable to parallelise grazing assays, e.g. between ciliates and algae. Finally, the theoretical possibility to measure particles of different sizes with a microplate nephelometer should be noted, a feature that has already been successfully exploited in flow cytometry [41].

### **Acknowledgements**

Thanks are due to Chloé Jollivet, Komlan Avia, Ian Probert, Pedro Murúa and Andrea Garvetto for supplying biological material. BMG Labtech is thanked for the generous loan of nephelometers and outstanding technical support.

### **Funding information**

This work was funded by the UK NERC IOF Pump-priming + award *GlobalSeaweed* (NE/L013223/1), the Genomia Fund (award HERDIR) and the project IDEALG (France: ANR-10-BTBR-04), and the H2020 project GENIALG (Grant Agreement No 727892).

### **Author contributions**

BC, MS, MMP and BJ performed most experiments; CR contributed her expertise in image analysis; BC, MV, YB and CMMG conceived the original research plan, with the assistance of JMC and CD. MV and CMMG supervised the experiments; BC, MMP and CMMG wrote the manuscript, with contributions of all other authors. All authors approved the final manuscript.

## Figure Legends

**Fig. 1. Principles of fluorometry (A), spectrophotometry (B) and nephelometry (C), with an overview of their respective pros and cons.**

**Fig. 2. Assessment of linearity and conservation of proportionality for dry weight measurement, nephelometry, fluorometry and spectrophotometry.**

Comparison of calibration curves obtained using a serial dilution of *E. siliculosus* tufts with dry weight measurement (A), nephelometry (B), fluorometry (C) and spectrophotometry (D). Three biological replicate wells were measured for each dilution of the *E. siliculosus* material (arbitrary unit on x axis) using the spectrometry methods (B-D, data plotted are average and SD). The algal tufts were then transferred into Eppendorf tubes, the medium was removed by pipetting, followed by overnight drying at 60°C. Due to the low amount of material present, the three replicates of each dilution had to be pooled into one tube. Tubes (one replicate per dilution) were then weighed three times with a precision scale, leading to the measurements (average and SD) shown in A. Note therefore that the standard deviations for the dry weight measurements (in A) are not directly comparable with those for the light-based measurements (B-D). A linear regression was calculated for each calibration curve. Furthermore, the deviation (D) between the observed slope and the dilution factor effectively applied was calculated with this formula: “(expected slope[x1, x2] – linear regression slope)/ expected slope[x1, x2]\*100”, where x1 and x2 are the two extreme points of the dilution series.

RNU: relative nephelometric unit. RFU: relative fluorescence unit. OD: optical density.

**Fig. 3. Comparison of nephelometry (purple), spectrophotometry (pink), and fluorometry (green) for the quantification of aquatic eukaryotes.** Calibration curves were obtained using the same approach as that illustrated in Fig. S2, i.e. using a serial dilution of different groups of algae and zoosporic fungi (“chytrids” *sensu lato*). Three biological replicate wells were measured for each

dilution. A linear regression was calculated for all the calibration curve for each optical methods (relative unit). The radar plot depicts the  $r^2$  of the resulting linear fits.

**Fig. 4. Non-invasive monitoring of *E. siliculosus* growth with spectrophotometry (black bars), nephelometry (grey bars), and fluorometry (white bars).** The photographs illustrate algal growth in one representative well. "Sat." indicates data saturation. For comparison purposes, all measurements are scaled in arbitrary units (AU) on the same Y axis as follows: RNU / 100 for nephelometry,  $OD * 10^3$  for spectrophotometry, and RFU \*10 for fluorometry. Bars represent the mean and SD of three biological replicates.

**Fig. 5. Detection of changes in *E. siliculosus* growth induced by abiotic factors.** Time-course in control conditions (full salinity and  $2 \mu\text{mol m}^{-2} \text{s}^{-1}$ ), and under hyposaline stress (10, 20 and 50% of normal salinity) or increased light ( $20 \mu\text{mol m}^{-2} \text{s}^{-1}$ ), as measured with nephelometry (A), fluorometry (B) and spectrophotometry (C). Data points represent the average and SD of three biological replicates.

**Fig. 6. Quantification of dead algal tissue.** A-C. Calibration curves obtained with serial dilutions of *E. siliculosus* using nephelometry (A), fluorometry (B) and spectrophotometry (C) after treatment with 1% sodium hypochlorite (white circles) or not (black circles). The unit on the x axis is arbitrary, with the highest quantity of *E. siliculosus* set to 1. D-E. Exemplary wells containing the same amount of algal biomass (three biological replicate), treated (D), or not (E), with 1% sodium hypochlorite. Scale bars: 200  $\mu\text{m}$ .

**Fig. 7. Non-invasive monitoring of disease progression in infected algal cultures.** A-C. Growth curves of *Macrocystis pyrifera* gametophytes infected by the intracellular biotrophic oomycete *Anisolpidium ectocarpii* as measured with nephelometry (A), fluorometry (B) and spectrophotometry (C). D-E. Representative microscopic field of views of a control (D) and an infected (E) *M. pyrifera* culture under

differential interference contrast (left hand side) and epifluorescence (right hand side), illustrating the phenotypic changes of infected cultures. Infected algal cells contain a parasitic thallus (E, arrowheads), surrounded by chestnut brown cell debris. At maturity, the oomycete releases zoospores through an exit tube (double arrowheads). Chlorophyll fluorescence collapses in infected cells from the early stages of the infection onwards. Scale bars: 20  $\mu\text{m}$ .

**Fig. 8. Quantification of spore release in kelp sporophytes, as a proxy for fertility measurement.**

**A-B.** The dark brown fertile area (sorus) of the kelp *S. latissima* (A) was photographed in field conditions and measured using image analysis (B). Scale bars: 1 cm. **C.** In parallel, a serial dilution of a calibrated spore suspension (with a Malassez cell) was measured with spectrophotometry (white circles, y axis on the right) and nephelometry (black circles, y axis on the left). For each concentration tested, three biological replicates were measured. **D.** Finally, the time-course of spore release was measured with nephelometry (D); the inset shows how kelp fragments (0.5x3 cm each) were disposed against the plate wall, in order to be fully immersed in the medium without interfering with the nephelometer's laser beam. The curves show two biological replicates (suffixed .1 and .2) for two individuals (A and B). The final RNU values at 150 min have been used to estimate the number of spores released per unit of fertile surface during the experiment. This value is multiplied by the total fertile surface to obtain a proxy for the individual's fertility.

RNU: relative nephelometric unit. OD: optical density at  $\lambda=230$  nm.

**Supplementary Figures**

**Fig. S1: Comparison of nephelometer, spectrophotometer and fluorometer accuracy.** The same sample of *E. siliculosus* filaments was measured ten times with each protocol (experimental replication, n=10). Whisker plots were drawn to visualise the data dispersion: the central thick line represents the median, the box contours represent the upper and lower quartiles, and dashed lines

show the minimum and maximum values measured. The standard deviation was calculated and normalised over the mean, for each method.

RNU: relative nephelometric unit. RFU: relative fluorescence unit. OD: optical density.

## Literature cited

- [1] R. Chandra, H.M. Iqbal, G. Vishal, H.-S. Lee, S. Nagra, Algal biorefinery: A sustainable approach to valorize algal-based biomass towards multiple product recovery, *Bioresource Technol*, (2019).
- [2] K. Sudhakar, R. Mamat, M. Samykano, W.H. Azmi, W.F.W. Ishak, T. Yusaf, An overview of marine macroalgae as bioresource, *Renew Sust Energ Rev*, 91 (2018) 165-179.
- [3] J.M. Cock, L. Sterck, P. Rouze, D. Scornet, A.E. Allen, G. Amoutzias, V. Anthouard, F. Artiguenave, J.M. Aury, J.H. Badger, B. Beszteri, K. Billiau, E. Bonnet, J.H. Bothwell, C. Bowler, C. Boyen, C. Brownlee, C.J. Carrano, B. Charrier, G.Y. Cho, S.M. Coelho, J. Collen, E. Corre, C. Da Silva, L. Delage, N. Delaroque, S.M. Dittami, S. Doulbeau, M. Elias, G. Farnham, C.M.M. Gachon, B. Gschloessl, S. Heesch, K. Jabbari, C. Jubin, H. Kawai, K. Kimura, B. Kloareg, F.C. Kupper, D. Lang, A. Le Bail, C. Leblanc, P. Lerouge, M. Lohr, P.J. Lopez, C. Martens, F. Maumus, G. Michel, D. Miranda-Saavedra, J. Morales, H. Moreau, T. Motomura, C. Nagasato, C.A. Napoli, D.R. Nelson, P. Nyvall-Collen, A.F. Peters, C. Pommier, P. Potin, J. Poulain, H. Quesneville, B. Read, S.A. Rensing, A. Ritter, S. Rousvoal, M. Samanta, G. Samson, D.C. Schroeder, B. Segurens, M. Strittmatter, T. Tonon, J.W. Tregear, K. Valentin, P. von Dassow, T. Yamagishi, Y. Van de Peer, P. Wincker, The *Ectocarpus* genome and the independent evolution of multicellularity in brown algae, *Nature*, 465 (2010) 617-621.
- [4] J. Collen, B. Porcel, W. Carre, S.G. Ball, C. Chaparro, T. Tonon, T. Barbeyron, G. Michel, B. Noel, K. Valentin, M. Elias, F. Artiguenave, A. Arun, J.M. Aury, J.F. Barbosa-Neto, J.H. Bothwell, F.Y. Bouget, L. Brillet, F. Cabello-Hurtado, S. Capella-Gutierrez, B. Charrier, L. Cladiere, J.M. Cock, S.M. Coelho, C. Colleoni, M. Czjzek, C. Da Silva, L. Delage, F. Denoeud, P. Deschamps, S.M. Dittami, T. Gabaldon, C.M.M. Gachon, A. Groisillier, C. Herve, K. Jabbari, M. Katinka, B. Kloareg, N. Kowalczyk, K. Labadie, C. Leblanc, P.J. Lopez, D.H. McLachlan, L. Meslet-Cladiere, A. Moustafa, Z. Nehr, P.N. Collen, O. Panaud, F. Partensky, J. Poulain, S.A. Rensing, S. Rousvoal, G. Samson, A. Symeonidi, J. Weissenbach, A. Zambounis, P. Wincker, C. Boyen, Genome structure and metabolic features in the red seaweed *Chondrus crispus* shed light on evolution of the Archaeplastida, *P Natl Acad Sci USA*, 110 (2013) 5247-5252.
- [5] N. Ye, X. Zhang, M. Miao, X. Fan, Y. Zheng, D. Xu, J. Wang, L. Zhou, D. Wang, Y. Gao, Y. Wang, W. Shi, P. Ji, D. Li, Z. Guan, C. Shao, Z. Zhuang, Z. Gao, J. Qi, F. Zhao, *Saccharina* genomes provide novel insight into kelp biology, *Nat Commun*, 6 (2015) 6986.
- [6] E.K. Hwang, F.L. Liu, K.H. Lee, D.S. Ha, C.S. Park, Comparison of the cultivation performance between Korean (Sugwawon No. 301) and Chinese strains (Huangguan No. 1) of kelp *Saccharina japonica* in an aquaculture farm in Korea, *Algae*, 33 (2018) 101-108.
- [7] R. Loureiro, C.M.M. Gachon, C. Rebours, Seaweed cultivation: potential and challenges of crop domestication at an unprecedented pace, *New Phytol*, 206 (2015) 489-492.
- [8] N. Robinson, P. Winberg, L. Kirkendale, Genetic improvement of macroalgae: status to date and needs for the future, *Journal of Applied Phycology*, 25 (2013) 703-716.
- [9] M. Valero, M.-L. Guillemin, C. Destombe, B. Jacquemin, C.M. Gachon, Y. Badis, A.H. Buschmann, C. Camus, S. Faugeron, Perspectives on domestication research for sustainable seaweed aquaculture, *Perspectives in Phycology*, (2017) 33-46.
- [10] J. Zhang, T. Liu, R. Feng, C. Liu, S. Chi, Genetic map construction and Quantitative Trait Locus (QTL) detection of six economic traits using an F2 population of the hybrid from *Saccharina longissima* and *Saccharina japonica*, *PLoS One*, 10 (2015) e0128588.
- [11] J.L. Collier, Flow cytometry and the single cell in phycology, *Journal of Phycology*, 36 (2000) 628-644.
- [12] L. Lefebvre-Legendre, Y. Choquet, R. Kuras, S. Loubery, D. Douchi, M. Goldschmidt-Clermont, A nucleus-encoded chloroplast protein regulated by iron availability governs expression of the photosystem I subunit PsaA in *Chlamydomonas reinhardtii*, *Plant Physiol*, 167 (2015) 1527-U1657.
- [13] M.J.W. Veldhuis, G.W. Kraay, Phytoplankton in the subtropical Atlantic Ocean: towards a better assessment of biomass and composition, *Deep-Sea Res Pt I*, 51 (2004) 507-530.

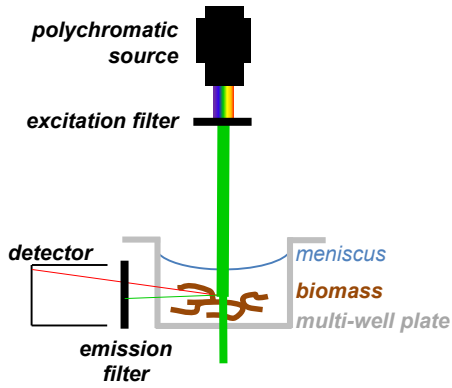


- [14] H. Berberoglu, L. Pilon, Experimental measurements of the radiation characteristics of *Anabaena variabilis* ATCC 29413-U and *Rhodobacter sphaeroides* ATCC 49419, *Int J Hydrogen Energ*, 32 (2007) 4772-4785.
- [15] A. Joubert, B. Calmes, R. Berruyer, M. Pihet, J.P. Bouchara, P. Simoneau, T. Guillemette, Laser nephelometry applied in an automated microplate system to study filamentous fungus growth, *Biotechniques*, 48 (2010) 399-404.
- [16] S. Pochon, P. Simoneau, S. Pigne, S. Balidas, N. Bataille-Simoneau, C. Campion, E. Jaspard, B. Calmes, B. Hamon, R. Berruyer, M. Juchaux, T. Guillemette, Dehydrin-like proteins in the necrotrophic fungus *Alternaria brassicicola* have a role in plant pathogenesis and stress response, *Plos One*, 8 (2013).
- [17] V. Redou, M. Navarri, L. Meslet-Cladiere, G. Barbier, G. Burgaud, Species richness and adaptation of marine fungi from deep-subseafloor sediments, *Appl Environ Microb*, 81 (2015) 3571-3583.
- [18] C. Butterwick, S. Heaney, J. Talling, A comparison of eight methods for estimating the biomass and growth of planktonic algae, *British Phycological Journal*, 17 (1982) 69-79.
- [19] C.M.M. Gachon, M. Strittmatter, D.G. Müller, J. Kleinteich, F.C. Küpper, Detection of differential host susceptibility to the marine oomycete pathogen *Eurychasma dicksonii* by real-time PCR: not all algae are equal, *Appl Environ Microb*, 75 (2009) 322-328.
- [20] C.M.M. Gachon, M. Strittmatter, Y. Badis, K.I. Fletcher, P. Van West, D.G. Müller, Pathogens of brown algae: culture studies of *Anisolpidium ectocarpii* and *A. rosenvingei* reveal that the Anisolpidiales are unflagellated oomycetes, *European Journal of Phycology*, 52 (2017) 133-148.
- [21] M. Strittmatter, T. Guerra, J. Silva, C.M. Gachon, A new flagellated dispersion stage in *Paraphysoderma sedebokerense*, a pathogen of *Haematococcus pluvialis*, *J Appl Phycol*, 28 (2016) 1553-1558.
- [22] C. Rad-Menendez, M. Gerphagnon, A. Garvetto, P. Arce, Y. Badis, T. Sime-Ngando, C.M.M. Gachon, Rediscovering *Zygorhizidium affluens* Canter: Molecular taxonomy, infectious cycle, and cryopreservation of a chytrid infecting the bloom-forming diatom *Asterionella formosa*, *European Journal of Phycology*, 50 (2015) 148-148.
- [23] R\_Core\_Team, R: A language and environment for statistical computing, (2013).
- [24] C. Rousseau, E. Belin, E. Bove, D. Rousseau, F. Fabre, R. Berruyer, J. Guillaumes, C. Manceau, M.A. Jacques, T. Boureau, High throughput quantitative phenotyping of plant resistance using chlorophyll fluorescence image analysis, *Plant Methods*, 9 (2013).
- [25] P.G. Falkowski, Light-shade adaptation in marine phytoplankton, *Primary productivity in the sea*, Springer1980, pp. 99-119.
- [26] A. Lehmuskero, M.S. Chauton, T. Boström, Light and photosynthetic microalgae: A review of cellular-and molecular-scale optical processes, *Progress in oceanography*, (2018).
- [27] M. Chioccioli, B. Hankamer, I.L. Ross, Flow cytometry pulse width data enables rapid and sensitive estimation of biomass dry weight in the microalgae *Chlamydomonas reinhardtii* and *Chlorella vulgaris*, *Plos One*, 9 (2014) e97269.
- [28] S. Van den Wyngaert, O. Vanholsbeeck, P. Spaak, B.W. Ibelings, Parasite fitness traits under environmental variation: disentangling the roles of a chytrid's immediate host and external environment, *Microbial ecology*, 68 (2014) 645-656.
- [29] M. Ermakova, T. Huokko, P. Richaud, L. Bersanini, C.J. Howe, D.J. Lea-Smith, G. Peltier, Y. Allahverdiyeva, Distinguishing the roles of thylakoid respiratory terminal oxidases in the cyanobacterium *Synechocystis* sp. PCC 6803, *Plant Physiol*, 171 (2016) 1307-1319.
- [30] A.M. Wood, R. Everroad, L. Wingard, Measuring growth rates in microalgal cultures, *Algal culturing techniques*, 18 (2005) 269-288.
- [31] K. Avia, S.M. Coelho, G.J. Montecinos, A. Cormier, F. Lerck, S. Mauger, S. Faugeron, M. Valero, J.M. Cock, P. Boudry, High-density genetic map and identification of QTLs for responses to temperature and salinity stresses in the model brown alga *Ectocarpus*, *Scientific reports*, 7 (2017) 43241.

- [32] F.L. Liu, Z.R. Shao, H.N. Zhang, J.D. Liu, X.L. Wang, D.L. Duan, QTL Mapping for frond length and width in *Laminaria japonica* Aresch (Laminariales, Phaeophyta) using AFLP and SSR Markers, *Mar Biotechnol*, 12 (2010) 386-394.
- [33] M. Bonhomme, O. Andre, Y. Badis, J. Ronfort, C. Burgarella, N. Chantret, J.M. Prosperi, R. Briskine, J. Mudge, F. Debelle, H. Navier, H. Miteul, A. Hajri, A. Baranger, P. Tiffin, B. Dumas, M.L. Pilet-Nayel, N.D. Young, C. Jacquet, High-density genome-wide association mapping implicates an F-box encoding gene in *Medicago truncatula* resistance to *Aphanomyces euteiches*, *New Phytol*, 201 (2014) 1328-1342.
- [34] S. Rasconi, M. Jobard, L. Jouve, T. Sime-Ngando, Use of Calcofluor White for detection, identification, and quantification of phytoplanktonic fungal parasites, *Appl Environ Microb*, 75 (2009) 2545-2553.
- [35] T.A. Klochkova, J.B. Shim, M.S. Hwang, G.H. Kim, Host-parasite interactions and host species susceptibility of the marine oomycete parasite, *Olpidiopsis* sp., from Korea that infects red algae, *Journal of Applied Phycology*, 24 (2012) 135-144.
- [36] M. Valero, S. Richerd, V. Perrot, C. Destombe, Evolution of alternation of haploid and diploid phases in life-cycles, *Trends Ecol Evol*, 7 (1992) 25-29.
- [37] J.M. Cock, O. Godfroy, N. Macaisne, A.F. Peters, S.M. Coelho, Evolution and regulation of complex life cycles: a brown algal perspective, *Curr Opin Plant Biol*, 17 (2014) 1-6.
- [38] S.M. Coelho, A.F. Peters, B. Charrier, D. Roze, C. Destombe, M. Valero, J.M. Cock, Complex life cycles of multicellular eukaryotes: New approaches based on the use of model organisms, *Gene*, 406 (2007) 152-170.
- [39] C. Destombe, J. Godin, M. Nocher, S. Richerd, M. Valero, Differences in response between haploid and diploid isomorphic phases of *Gracilaria verrucosa* (Rhodophyta, Gigartinales) exposed to artificial environmental conditions, *Hydrobiologia*, 261 (1993) 131-137.
- [40] B.R. Robertson, D.K. Button, A.L. Koch, Determination of the biomasses of small bacteria at low concentrations in a mixture of species with forward light scatter measurements by flow cytometry, *Appl Environ Microb*, 64 (1998) 3900-3909.
- [41] H.B. Steen, Flow cytometer for measurement of the light scattering of viral and other submicroscopic particles, *Cytom Part A*, 57a (2004) 94-99.

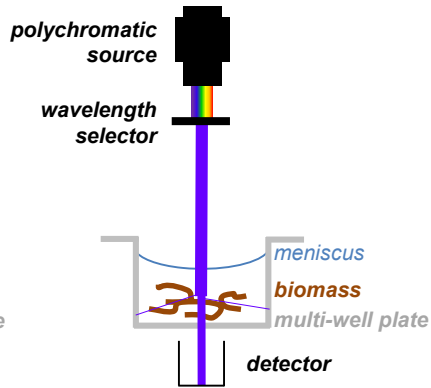
# Fig. 1

## A. Fluorometry



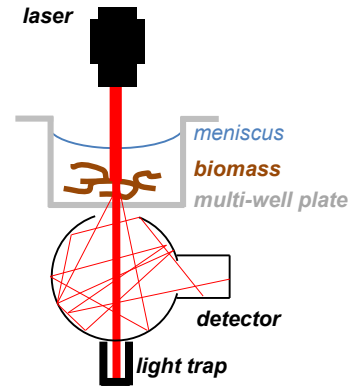
colour multiplexing possible  
insensitive to meniscus  
dynamic range ++

## B. Spectrophotometry (optical density)



wavelength selectable  
insensitive to meniscus  
dynamic range +++

## C. Nephelometry

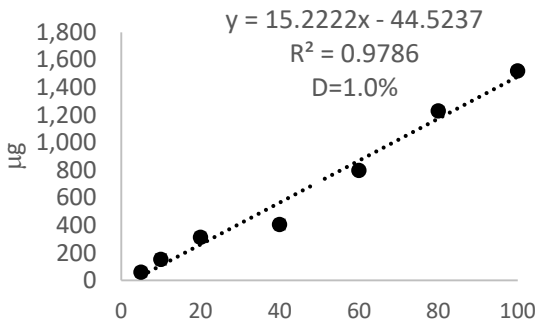


colour-independent  
sensitive to meniscus  
dynamic range +++

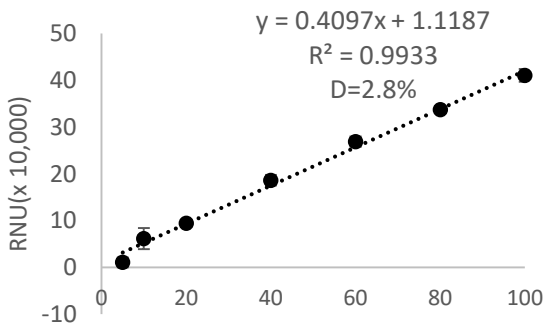
Fig. 1. Principles of fluorometry (A), spectrophotometry (B) and nephelometry (C), with an overview of their respective pros and cons.

# Fig. 2

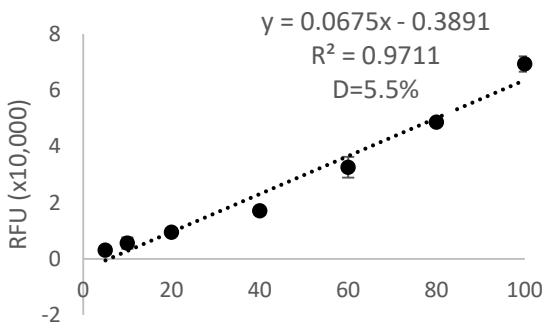
## A. Dry weight



## B. Nephelometry



## C. Fluorometry



## D. Spectrophotometry

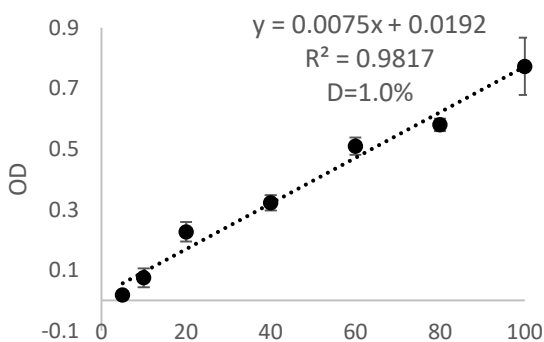


## Fig. 2. Assessment of linearity and conservation of proportionality for dry weight measurement, nephelometry, fluorometry and spectrophotometry.

Comparison of calibration curves obtained using a serial dilution of *E. siliculosus* tufts with dry weight measurement (A), nephelometry (B), fluorometry (C) and spectrophotometry (D). Three biological replicate wells were measured for each dilution of the *E. siliculosus* material (arbitrary unit on x axis) using the spectrometry methods (B-D, data plotted are average and SD). The algal tufts were then transferred into Eppendorf tubes, the medium was removed by pipetting, followed by overnight drying at 60°C. Due to the low amount of material present, the three replicates of each dilution had to be pooled into one tube. Tubes (one replicate per dilution) were then weighed three times with a precision scale, leading to the measurements (average and SD) shown in A. Note therefore that the standard deviations for the dry weight measurements (in A) are not directly comparable with those for the light-based measurements (B-D). A linear regression was calculated for each calibration curve. Furthermore, the deviation (D) between the observed slope and the dilution factor effectively applied was calculated with this formula:  $\{(\text{expected slope}[x_1, x_2] - \text{linear regression slope}) / \text{expected slope}[x_1, x_2] * 100\}$ , where  $x_1$  and  $x_2$  are the two extreme points of the dilution series.

RNU: relative nephelometric unit. RFU: relative fluorescence unit. OD: optical density.

# Fig. 3

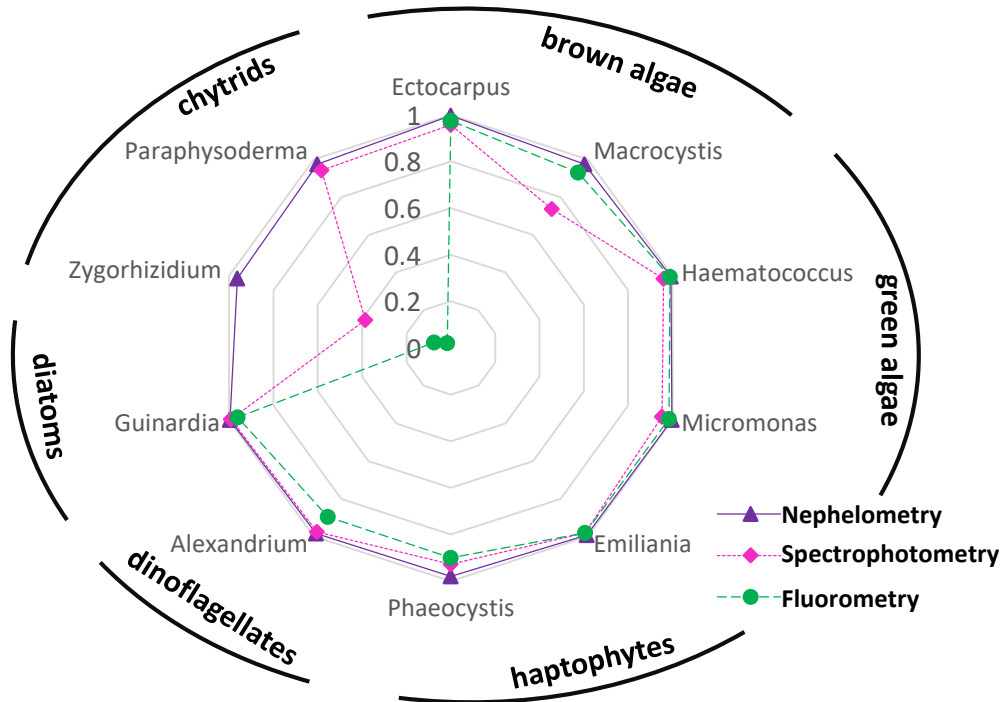


**Fig. 3. Comparison of nephelometry (purple), spectrophotometry (pink), and fluorometry (green) for the quantification of aquatic eukaryotes.** Calibration curves were obtained using the same approach as that illustrated in Fig. 2, i.e. using a serial dilution of different groups of algae and zoosporic fungi (“chytrids” *sensu lato*). Three biological replicate wells were measured for each dilution. A linear regression was calculated for all the calibration curve for each optical methods (relative unit). The radar plot depicts the  $r^2$  of the resulting linear fits.

# Fig. 4

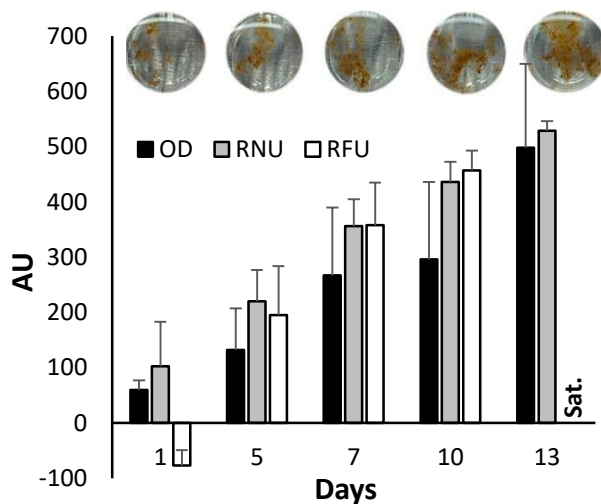


**Fig. 4. Non-invasive monitoring of *E. siliculosus* growth with spectrophotometry (black bars, nephelometry (grey bars), and fluorometry (white bars)).** The photographs illustrate algal growth in one representative well. "Sat." indicates data saturation. For comparison purposes, all measurements are scaled in arbitrary units (AU) on the same Y axis as follows: RNU / 100 for nephelometry, OD \* 10<sup>3</sup> for spectrophotometry, and RFU \*10 for fluorometry. Bars represent the mean and SD of three biological replicates.

# Fig. 5

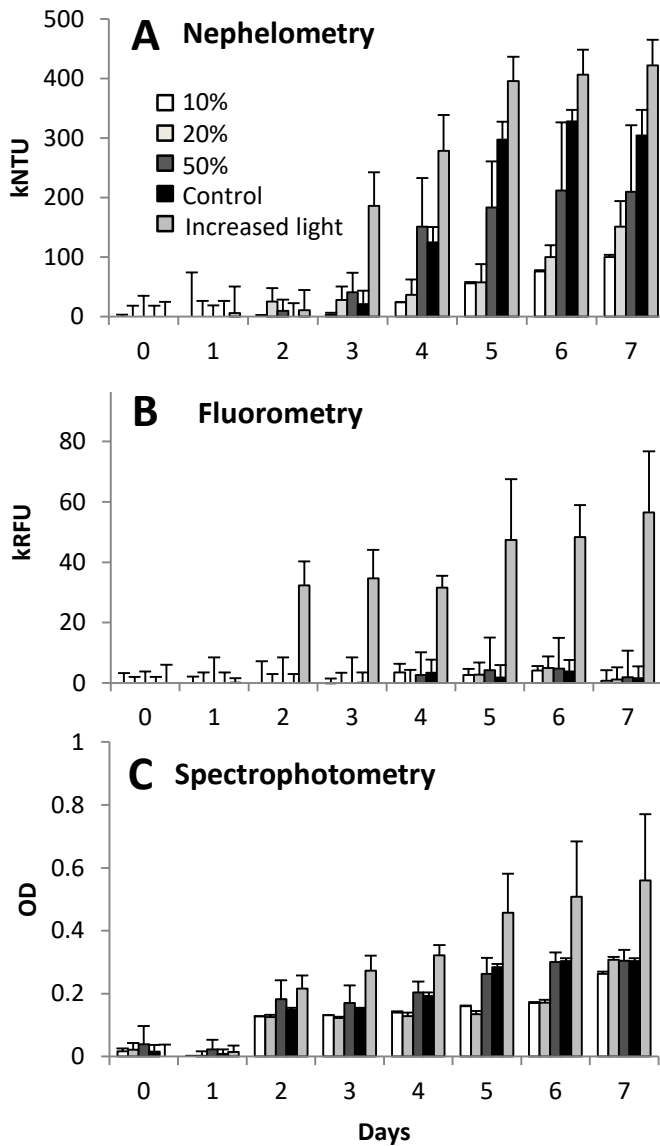


**Fig. 5. Detection of changes in *E. siliculosus* growth induced by abiotic factors.** Time-course in control conditions (full salinity and  $2 \mu\text{mol m}^{-2} \text{s}^{-1}$ ), and under hyposaline stress (10, 20 and 50% of normal salinity) or increased light ( $20 \mu\text{mol m}^{-2} \text{s}^{-1}$ ), as measured with nephelometry (A), fluorometry (B) and spectrophotometry (C). Data points represent the average and SD of three biological replicates.

# Fig. 6

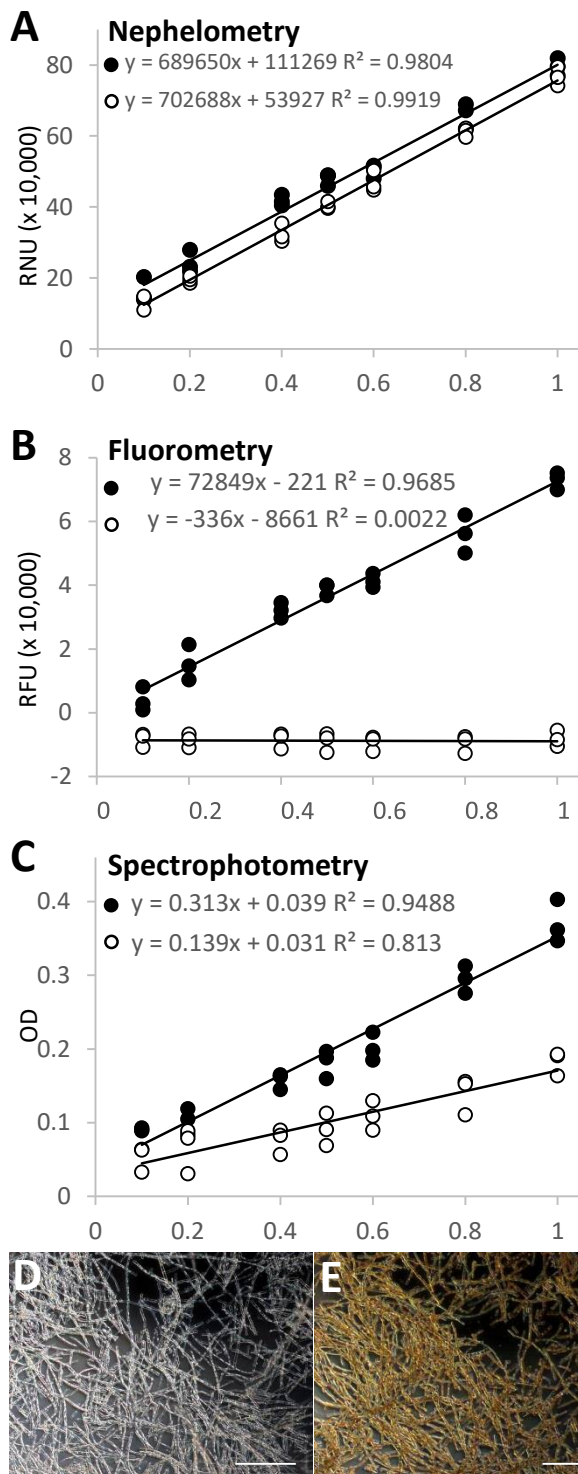


**Fig. 6. Quantification of dead algal tissue.** A-C. Calibration curves obtained with serial dilutions of *E. siliculosus* using nephelometry (A), fluorometry (B) and spectrophotometry (C) before (black circles) and after treatment with 1% sodium hypochlorite (white circles) or not (black circles). The unit on the x axis is arbitrary, with the highest quantity of *E. siliculosus* set to 1. D-E. Exemplary wells containing the same amount of algal biomass (three biological replicate), treated (D), or not (E), with 1% sodium hypochlorite. Scale bars: 200  $\mu\text{m}$ .



# Fig. 7

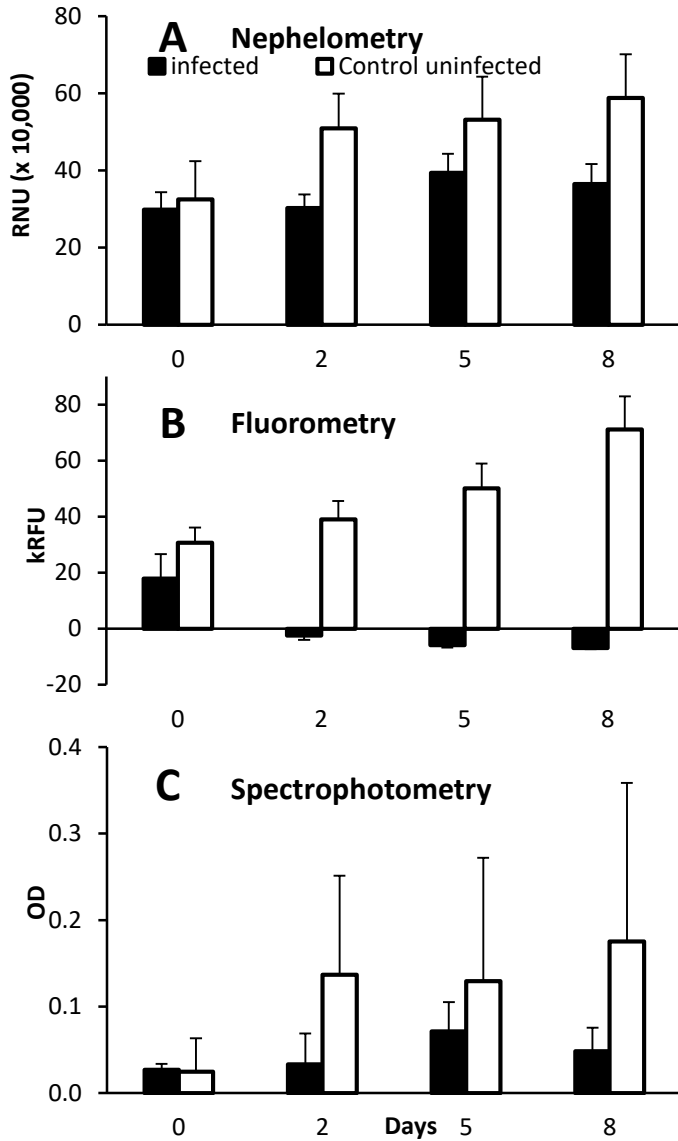


**Fig. 7. Non-invasive monitoring of disease progression in infected algal cultures.** A-C. Biomass of *Macrocyctis pyrifera* gametophytes infected by the intracellular biotrophic oomycete *Anisolpidium ectocarpii* as measured with nephelometry (A), fluorometry (B) and spectrophotometry (C). D-E. Representative microscopic field of views of a control (D) and an infected (E) *M. pyrifera* culture under differential interference contrast (left hand side) and epifluorescence (right hand side), illustrating the phenotypic changes of infected cultures. Infected algal cells contain a parasitic thallus (E, arrowheads), surrounded by chestnut brown cell debris. At maturity, the oomycete releases zoospores through an exit tube (double arrowheads). The Chlorophyll fluorescence collapses in infected cells, from the early stages of the infection onwards. Scale bars: 20  $\mu$ m.

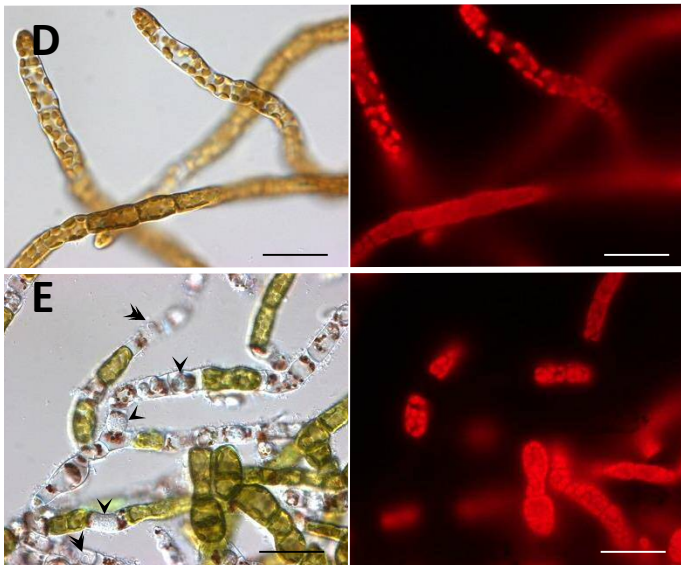


# Fig. 8

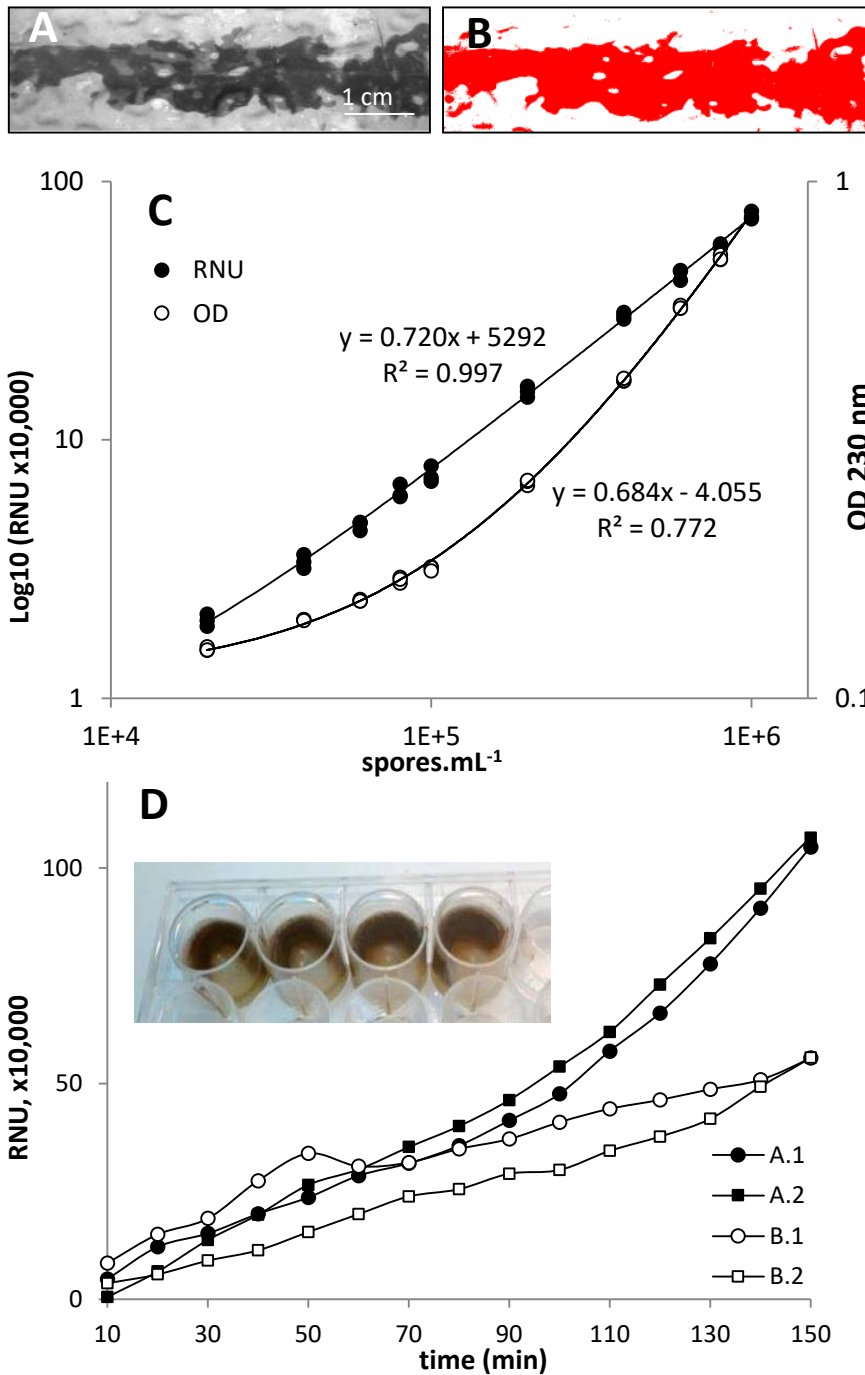


**Figure 8: Quantification of spore release in kelps, as a proxy for fertility measurement.**

**A-B.** The dark brown fertile area (sorus) of the kelp *S. latissima* (A) was photographed in field conditions, and measured using image analysis (B). Scale bars: 1 cm. **C.** In parallel, a serial dilution of a calibrated spore suspension (with a Malassez cell) was measured with spectrophotometry (white circles, y axis on the right) and nephelometry (black circles, y axis on the left). For each concentration tested, three biological replicates were measured. **D.** Finally, the time-course of spore release was measured with nephelometry (D); the inset shows how kelp fragments (0.5x3 cm each) were disposed against the plate wall, in order to be fully immersed in the medium without interfering with the nephelometer's laser beam. The curves show two biological replicates (suffixed .1 and .2) for two individuals (A and B). The final RNU values at 150 min have been used to estimate the number of spores released per unit of fertile surface during the experiment. This value is multiplied by the total fertile surface to obtain a proxy for the individual's fertility.

RNU: relative nephelometric unit. OD: optical density at  $\lambda=230$  nm.

# Fig. S1

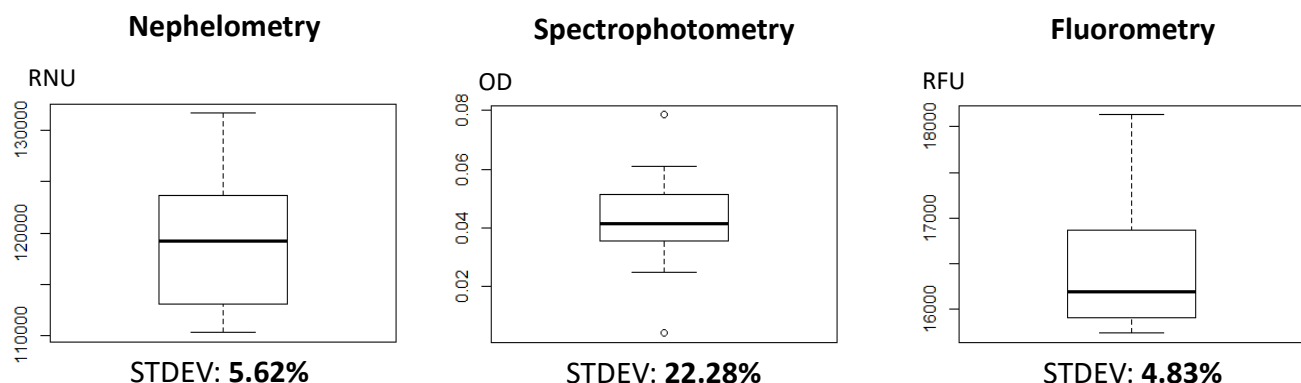


**Figure S1: Comparison of nephelometer, spectrophotometer and fluorometer accuracy.** The same sample of *E. siliculosus* filaments was measured ten times with each protocol (experimental replication, n=10). Whisker plots were drawn to visualise the data dispersion: the central thick line represents the median, the box contours represent the upper and lower quartiles, and dashed lines show the minimum and maximum values measured. The standard deviation (STDEV) was calculated and normalised over the mean, for each method.

RNU: relative nephelometric unit. RFU: relative fluorescence unit. OD: optical density.